

## OS4-6

ISS 実験で明らかになった微粒化における表面張力波の  
役割The role of capillary waves in atomization revealed by  
ISS experiments新城 淳史<sup>1</sup>, 梅村 章<sup>2</sup>Junji SHINJO<sup>1</sup> and Akira UMEMURA<sup>2</sup>

1 島根大学次世代たたら協創センター, Next Generation Tatara Co-Creation Centre, Shimane University

2 名古屋大学航空宇宙工学専攻, Department of Aerospace Engineering, Nagoya University

### 1. Introduction

Liquid atomization is widely used in engineering applications such as engine combustion, spray coating, pharmaceutical production etc. Surface tension plays a significant role in the development of liquid/gas interface instability and droplet pinch-off. In order to observe and measure detailed dynamics, a liquid jet is issued from a nozzle. In the conventional notion, the jet will disintegrate due to noise fluctuations in the jet which are due to some unidentified external sources in the upstream region. However, in our proposal, the trigger for disintegration is intrinsically generated spontaneously from inside the jet. Here, the jet tip contraction due to surface tension generates capillary waves which travel upstream, and a destabilizing mechanism due to reflection by the liquid velocity profile leads to final pinch-off. Experimentally on the ground, the gravity adds unnecessary acceleration to the jet and alters the dynamics. Therefore, the microgravity environment on the ISS is ideal in observing pure effects of capillary waves induced by surface tension.

Here, ISS experimental results in the Atomization Project are reported following the reference<sup>1)</sup>. The experiments were conducted to validate our proposal that a real finite-length liquid jet can spontaneously disintegrate due to its intrinsic self-destabilizing mechanism induced by capillary waves. Thanks to long experimental time unaffected by the gravity on the ISS, dynamic evolution of capillary waves and subsequent atomization was observed in detail. The findings in the experiments are used in modeling atomization, which will contribute to improving efficiency and cleanness in engine combustion.

### 2. Experimental Setup

Figure 1 shows the schematic of the experimental setup on the ISS<sup>1)</sup>. A slow water jet is issued from a nozzle controlled by the piston motion. A high-speed camera captures the detailed interface dynamics with the back light from an LED light sheet. The piston syringe is changeable and the nozzle shape can be varied accordingly. In this experiment, an orifice shape (no nozzle length) is also used.

Hereafter, the jet speed is normalized by the tip contraction velocity  $V = \sqrt{\sigma/\rho a}$  where  $\sigma$  is the surface tension coefficient,  $\rho$  is the water density and  $a$  is the injector (nozzle or orifice) radius. The injector radius used here is  $a=0.4, 0.55, 0.8$  and  $1.0$ mm and the nozzle length is 30mm and 120mm, and for the orifice it is 0 mm. The jet speed is varied during the experiment in several patterns<sup>1)</sup>.

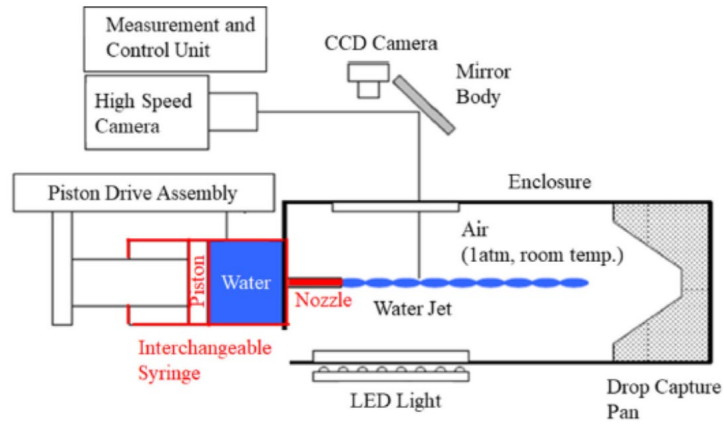


**Fig. 1** Schematic of the experimental apparatus<sup>1)</sup>

### 3. Results and Discussion

Figure 2 shows a typical sequence of images obtained in the present experiments. Water is injected from the left side and disintegrates into droplets after some time. The local maximum points of the surface shape are extracted from these images and used for analysis. The red lines in the figure indicate the local maximum and the green lines indicate the jet front position.



**Fig. 2** Typical experimental images<sup>1)</sup>

Figure 3 shows the time sequence of the maximum points for several jet issue speeds ( $U/V=1.60, 1.84, 2.00, 3.15$  and  $4.33$ ). The nozzle radius is  $a=0.4\text{mm}$  and nozzle length is  $120\text{mm}$ . The red line indicates the tip position. The nozzle jet region with the inclined profiles of maximum points has the same structure as that of the orifice jet. Inside the nozzle, the velocity profile becomes parabolic due to the wall friction. After injected into the free space, the velocity profile relaxes to a flat plug flow profile, similarly to that of an orifice flow. Therefore, the upstream region in the nozzle jet plays the same role as the orifice reflection. At the same time, hysteresis behavior in  $1 < U/V < 2$  is observed when the issue speed is increased and decreased (not shown here), which indicates that the jet disintegration is affected by the past history, not by the one-way mechanism of conventional notion. The short-length breakup mode occurs in the velocity relaxation region when the speed is increased, before the long-length breakup mode occurs. The velocity dependence of the nozzle jets is similar to that of orifice jets. Under the slow jet speed conditions, liquid accumulation at the jet tip due to tip contraction primarily causes disintegration. Tip contraction generates capillary waves which travel upstream and reflect at the nozzle exit. The reflected waves determine the timing of jet disintegration.

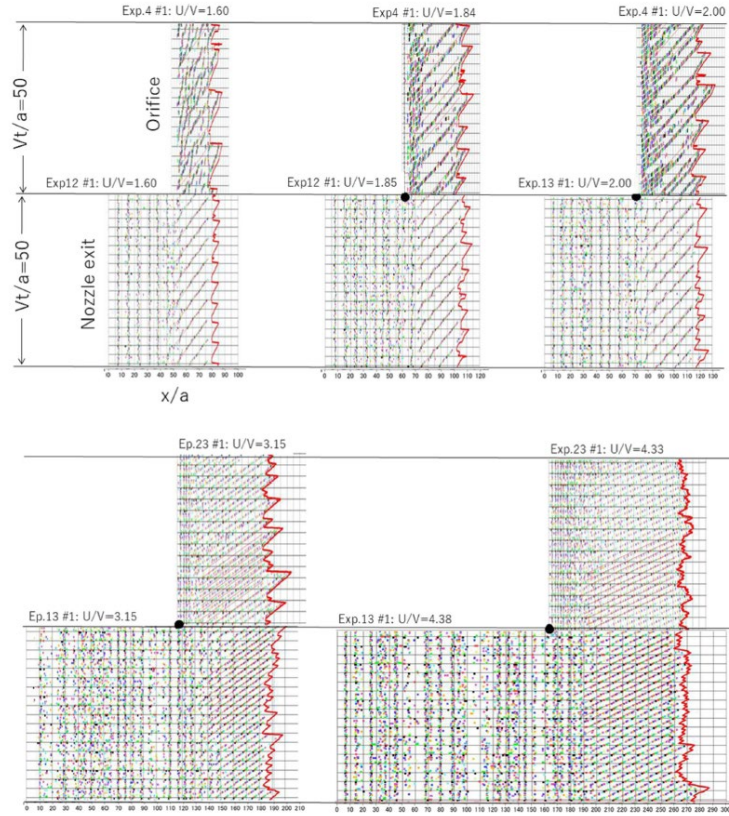


Fig. 3 Temporal behavior of maximum points for orifice and  $a=0.4\text{mm}$   $l=120\text{mm}$  nozzle<sup>1)</sup>

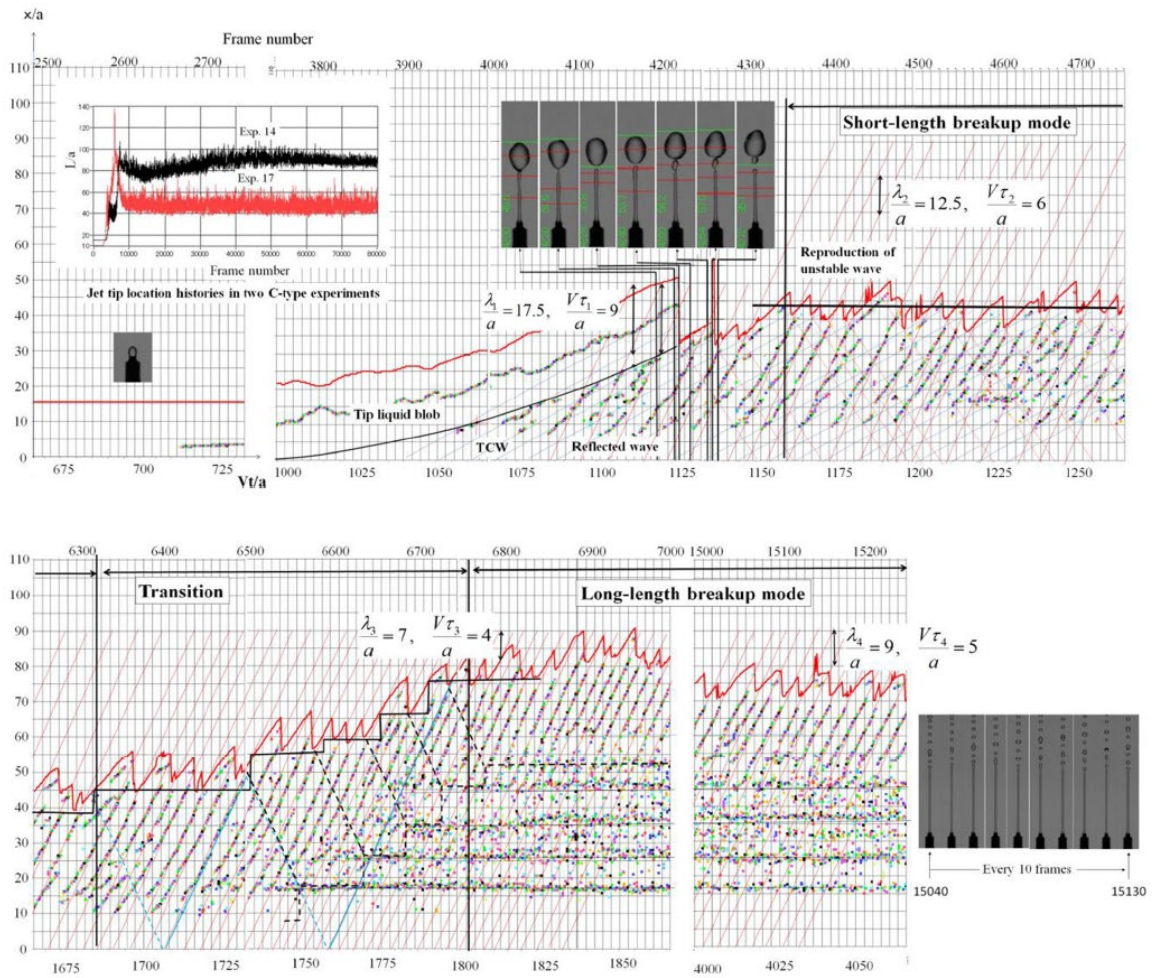


Fig. 4 Temporal behavior of maximum points for  $a=0.4\text{mm}$   $l=120\text{mm}$  nozzle at constant  $U/V=1.61$ <sup>1)</sup>

In the hysteresis behavior, transition to the long-length breakup mode occurs. Next, this behavior is shown with the case of  $a=0.4\text{mm}$   $l=120\text{mm}$  nozzle with  $U/V=1.61$ . The velocity is set constant to realize steady jet disintegration. In this long-length breakup mode, unstable wave generation is due to elongation of tip capillary waves after reflection. Long waves make the surface deformation longer and the surface tension in the generation line direction weaker, which leads to breakup.

Figure 4 shows the transition from the initial short-length breakup mode to the long-length breakup mode. Since the issue speed is kept constant, initially the short-length breakup mode appears after the free jet formation period. Here, synchronization of disintegration and capillary wave behavior is attained and the same behavior as the one in Fig. 3 occurs. If some mismatching due to the past disintegration history occurs, there will be a chance for reflected unstable waves to be longer. In Fig.4, the step-like increase in the breakup length is observed, as shown by the black solid line. Accordingly, in the upstream region, non-wave-like maximum point trajectories can be found, as shown by the black dashed line. This situation is due to a region, which we call "S-location", where the surface velocity relaxation makes the velocity profile flat and elongated unstable waves are generated on the surface. These waves travel downstream and finally lead to breakup. As a result, this velocity relaxation region acts as an orifice, and the breakup length is the sum of velocity relaxation region and orifice jet breakup length.

#### 4. Conclusions

Thanks to long experimental time under the microgravity environment on the ISS, detailed behavior of jet disintegration has been well observed. It has been found that jet disintegration is spontaneously caused by tip capillary wave generation due to surface tension. The short-length breakup mode occurs within the velocity relaxation region of a nozzle flow. Therefore, the jet speed dependence is similar for both nozzle and orifice jets. At a small speed, liquid accumulation by tip contraction leads to disintegration with the timing determined by tip capillary wave reflection back from the nozzle. Transition to the long-length breakup mode is also discussed. The velocity relaxation region plays an important role in producing elongated reflected waves. The elongated waves finally lead to disintegration in the downstream. The present experiments have confirmed the concept of jet disintegration caused by tip capillary wave generation, which is self-induced and spontaneous in every finite-length liquid jet.

#### References

- 1) A. Umemura, J. Osaka, J. Shinjo, Y. Nakamura, S. Matsumoto, M. Kikuchi, T. Taguchi, H. Ohkuma, T. Dohkojima, T. Shimaoka, T. Sone, H. Nakagami, W. Ono: *Microgravity Sci. Technol.*, **32** (2020) 369.



© 2021 by the authors. Submitted for possible open access publication under the terms and conditions of the Creative Commons Attribution (CC BY) license (<http://creativecommons.org/licenses/by/4.0/>).